

OPTIMISATION OF THE TRI-AURAL SYSTEM, DETECTION AND IDENTIFICATION OF DIFFERENT REFLECTORS

Gabriel Pires, Nelson Martins, Rui Almeida, F. Moita, Urbano Nunes, A. T. de Almeida
 Institute of Systems and Robotics, and Electrical Engineering Department, University of Coimbra,
 3000 Coimbra, Portugal. E-mail: {gpIRES , urbano}@isr.uc.pt

ABSTRACT

Two different systems composed by three Time-of-Flight (TOF) ultrasonic sensors lined up (tri-aural system) are employed to recognise planes, edges and curved reflectors in a 2 1/2 D world. These systems can be useful for sonar map building and robot navigation. A study of these two systems is made in order to find out which of them has the better performance. The best configuration of the tri-aural system (distance between transducers and orientation of lateral transducers) for recognition and perception purposes is investigated. The results presented in this paper were obtained by MATLAB simulations and real experiments.

1 INTRODUCTION

Ultrasonic sensors have been widely used to determine the proximity of objects and have been useful to implement sonar systems for obstacle detection and avoidance [9], robot navigation [6, 8] and sonar map building [7]. These sensors are low cost and easy to manage which explains their widespread use. This paper addresses the recognition problem of 2D geometrical features. It describes two tri-aural (TA) systems designated TA-I and TA-II. The geometric configurations of both TA systems are identical but while TA-I has the central sensor acting as transmitter/receiver (T/R) and the lateral sensors acting as receivers (R), TA-II has all three sensors acting as T/R sequentially fired up.

2 DESCRIPTION OF THE TRI-AURAL SYSTEM

Both systems consist of three Polaroid transducers resonant at $f_0=49,4$ KHz. Each transducer can work simultaneously as transmitter/receiver or simply as receiver. The beam width of the transducers is approximately 20° (angle ϕ in Figure 1). Lateral transducers can take different positions and orientations in respect to the central transducer. In our setup the distances d_1 and d_2 (see Figure 1) can range from 5 to 15 cm and the orientation angle ϕ can vary from 0° to 15° . The normal mode of operation of an ultrasonic ranging sensor consists of transmitting a pulse and measuring the time it takes to the first echo to return (TOF method). The TOF t_0 of the ultrasound pulse allows us to determine the distance ($m/2$)

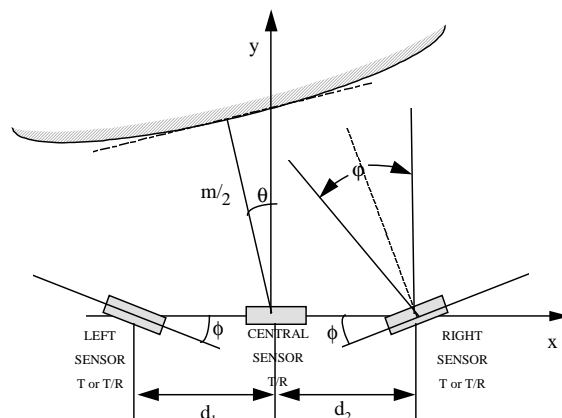


Figure 1. 2D tri-aural sensor arrangement. Lateral sensors actuate simply as R or T/R accordingly we are dealing with the TA-I or TA-II system.

between the transducer and the reflector:

$$\frac{m}{2} = \frac{ct_0}{2} \quad (1)$$

where c is the speed of sound in air. The array of transducers is mounted on a 2 DOF (degrees of freedom) high precision mechanical structure with linear and angular precision of 0.1 mm and 0.01 degrees respectively (see Figure 3).

3 REFLECTORS GEOMETRY

We consider only the case of curved reflectors [1]. A plane is modelled by an infinite radius of curvature and an edge by a zero radius of curvature. Corners will not be studied because

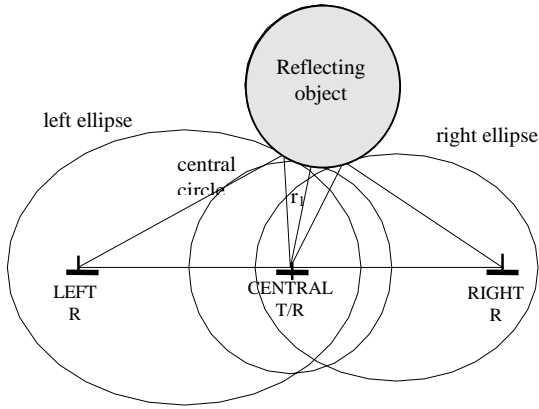


Figure 2. Geometric model of the TA-I system.

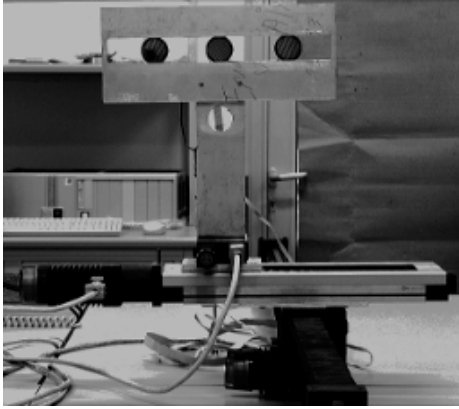


Figure 3. Tri-aural system mounted on a 2 DOF (degrees of freedom) high precision mechanical structure.

as it was shown in [4], corners cannot be distinguished from planes if we just have access to TOF measures. However, some researchers [2,3] have reached a successful differentiation of corners by studying amplitudes of the echo signals.

4 TA GEOMETRIC MODELS

The position and the radius of curvature of circular reflectors can be obtained combining the information of the three sensors of the TA system. In the next two subsections we present observation models of TA-I and TA-II systems [1,5].

4.1 Observation model of TA-I system

An observation model of TA-I system is developed in this section. Consider for that Figures 2 and 4. Let m_1 , m_2 and m_3 denote respectively the distances defined by the following paths: central sensor-reflector-central sensor, central sensor - reflector - left sensor, central sensor-reflector-right sensor. The locus

of points for which the distance m_1 is constant is

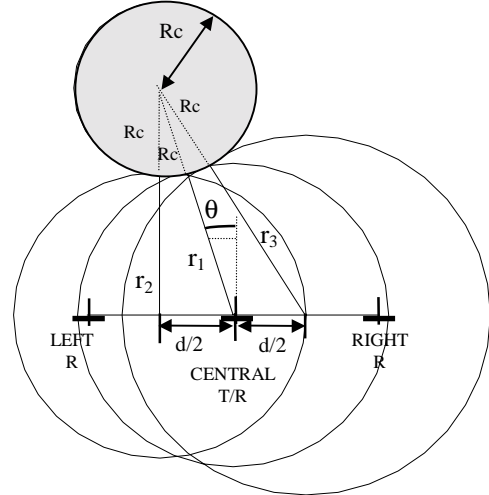


Figure 4. Approximation model of the TA-I system.

a circle and, the locus of points for which m_2 (m_3) is constant is an ellipse with focus at the central and left (right) transducers as depicted in Figure 2. To simplify calculations, these ellipses can be approximated by circles with centres halfway between the two focus, and their radius equal to the length of the semiminor axes of the ellipses [1] as shown in Figure 4. If m_1 , m_2 and m_3 denote the measures of central, left and right sensors, respectively, the radius of the circles, represented in Figure 4, are given by

$$r_1 = \frac{m_1}{2}, r_2 = \sqrt{\frac{m_2^2 - d^2}{4}}, r_3 = \sqrt{\frac{m_3^2 - d^2}{4}} \quad (2)$$

where d denotes the distance between the central and the lateral transducers. For the conditions presented in Figure 4, the location (θ, r_1) and the radius of curvature (Rc) can be expressed mathematically as follows:

$$Rc = \frac{2r_1^2 - r_2^2 - r_3^2 + d^2/2}{2(r_2 + r_3 - 2r_1)} \quad (3)$$

and

$$\theta = \arcsin\left(\frac{r_3^2 - r_2^2 + 2Rc(r_3 - r_2)}{2d(r_1 + Rc)}\right) \quad (4)$$

It was observed in practice a unsatisfactory behaviour of equation 3. This fact lead us to perform a sensitivity analysis of that equation. For this study we consider the following reference situation: $\theta=0^\circ$, $\phi=0^\circ$, $d_1=d_2=15$ cm, $\phi=20^\circ$ and a planar object reflector placed at a distance of 1 m. For this configuration we

obtain the theoretical values of $m_1=2$ m and $m_2=m_3=2.005618$ m. Introducing the theoretical values of m_2 and m_3 in equation 3, and taking m_1

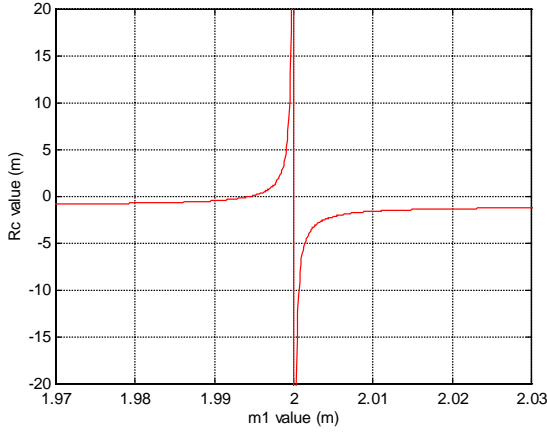


Figure 5. R_c vs m_1 for the TA-I system.

as a variable we obtain the results for R_c shown in Figure 5. We can observe that when m_1 takes the correct value of 2 m, R_c is infinite. This is the expected result since $R_c=\infty$ defines a planar reflector. However we can also observe that if m_1 suffers a small error of $\cong 5$ mm, a plane will be confounded by an edge (the two limit situations). The results show that equation 3 is very sensitive with variable m_1 . Since angle θ , equation 4, is a function of R_c , it is also very sensitive with errors of m_1 .

4.2 Observation model of TA-II system

All sensors of the TA-II system work in the T/R mode, and are sequentially fired up. In this case the locus of points, for which m_1 , m_2 and m_3 are constants, are circles with centres on the respective transducers, as shown in Figure 6. The radius of these circles are:

$$r_1 = \frac{m_1}{2}, r_2 = \frac{m_2}{2}, r_3 = \frac{m_3}{2} \quad (5)$$

The geometric model leads us to the following equations for R_c and θ :

$$R_c = \frac{2r_1^2 - r_2^2 - r_3^2 + 2d^2}{2(r_2 + r_3 - 2r_1)}, \quad \theta = \frac{r_3^2 - r_2^2}{4dr_1} \quad (6)$$

which are easily deduced with no need of approximations. Similarly to the study done in the previous section, we have made a sensitivity analysis of R_c equation 6. The results of this analysis are depicted graphically in Figure 7. If we attend to Figures 5 and 7 we can note that the R_c curve function of m_1 is smoother in Figure 7. In fact, the difference between m_1 values for $R_c=\infty$ and $R_c=0$ is approximately 5

times larger (2,5 cm) than for the previous case, i.e., R_c equation 6 it is less sensitive to errors of m_1 . This result predicts that the TA-II system

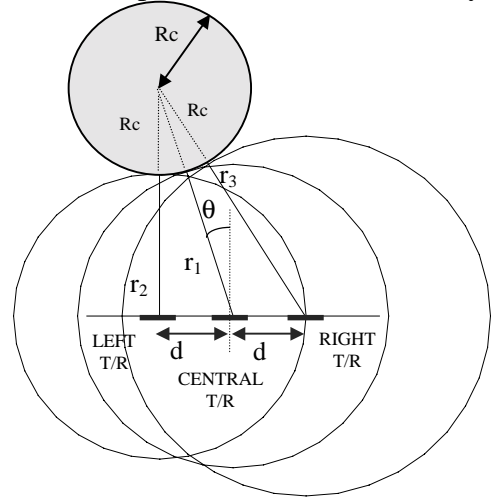


Figure 6. Geometric model of the TA-II system.

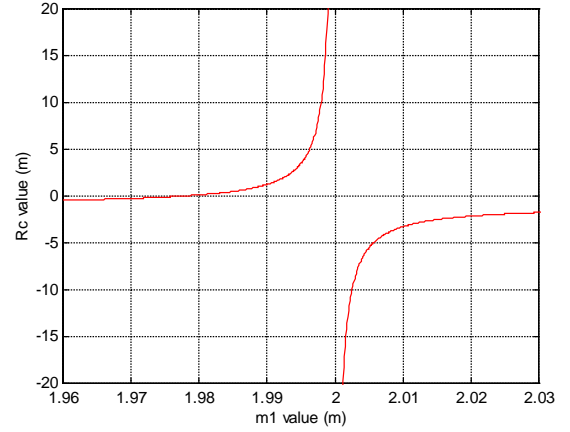


Figure 7. R_c vs m_1 for the TA-II system.

will have a better performance in the real world than the TA-I system.

4.3 Orientation of planar reflectors

Another method to find the orientation of a plane is discussed in this section. If we know in advance that the reflector is planar, then its orientation could be found using only two measures, one from the central sensor and the other from one lateral sensor. The method consists of determining a common tangent to the central circle and to the lateral ellipse, as shown in Figure 8. From the geometrical model shown in Figure 8, we have deduced that the angle θ , of a planar reflector, can be expressed as follows:

$$\theta = \frac{180 \times \text{atan}(m)}{\pi} \quad (7)$$

where m is given by

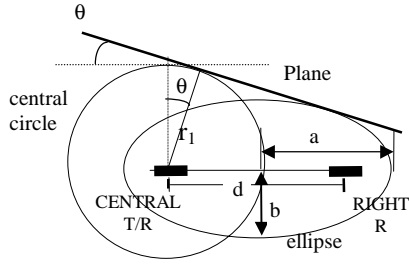


Figure 8. Orientation determination of planar reflectors with the TA-I system.

$$m = \frac{\frac{b}{a}(d - 2x)}{2\sqrt{a^2 - \left(x - \frac{d}{2}\right)^2}} \quad (8)$$

with

$$x = \frac{-x_1 + \sqrt{x_1^2 - 4x_0x_2}}{2x_0}$$

where

$$\begin{aligned} x_0 &= \frac{1}{a^2} \left(4a^2r_1^2 + b^2(d^2 - 4r_1^2) \right) \\ x_1 &= \frac{1}{a^2} d \left(4a^2(b^2 - r_1^2) + b^2(4r_1^2 - d^2) \right) \\ x_2 &= \frac{1}{4a^2} \left(16a^4(b^2 - r_1^2) - 4a^2d^2(2b^2 - r_1^2) + b^2d^2(d^2 - 4r_1^2) \right) \end{aligned}$$

With this method we need only a pair of measures (m_1, m_2) or (m_1, m_3) to determine the orientation of planar reflectors. This method will permit, as we shall see farther on, to augment the range of detectable orientations by the TA-I system.

5 PERFORMANCE OF TA-I AND TA-II SYSTEM vs SPATIAL CONFIGURATION

5.1 Distance to the reflector

Figure 9 shows the values of m_2 for the two limit situations, $Rc=0$ and $Rc=\infty$. We can observe that the differences between the m_2 values for a plane and an edge are larger in the case of TA-II system. However these differences decrease for larger distances, for both TA-I and TA-II systems. Larger

differences between the m_2 measures lead to greater insensitivity of Rc to errors of m_2 .

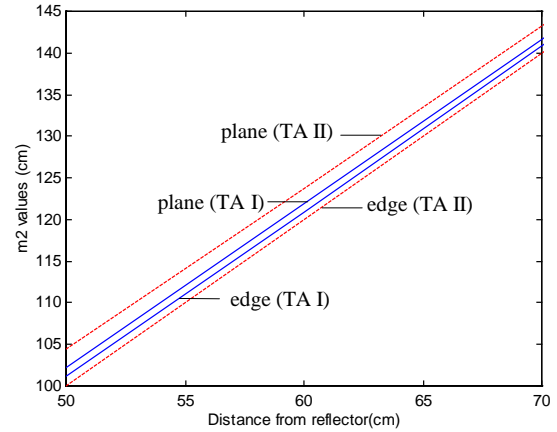


Figure 9. m_2 measures for a plane and an edge (-TA-I system ; -- TA-II system)

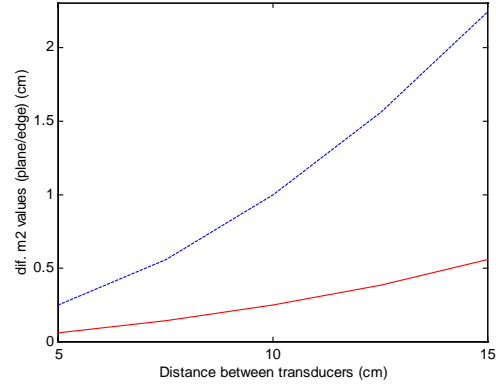


Figure 10. Differences between m_2 values for a plane and an edge (-TA I ; --TA II).

5.2 Distance between transducers

The differences between m_2 measures for a plane and an edge vary with the distance between transducers as it can be observed in Figure 10. These differences are quite large for large distances between transducers.

5.3 Radius of curvature vs orientation

The equation 3 gives different Rc values as a function of the orientation θ . It gives only correct Rc values for the case of $\theta=0$. Figure 11 shows this bad behaviour of model (3) for the case of an edge reflector. In the contrary the model (6) (TA-II system) gives correct Rc values independently of the θ values (obviously, in the observation range $\theta \in [-10^\circ, +10^\circ]$).

5.4 Increasing the TA-I system visibility range

This study was made just for planar reflectors with the aim of increasing the range of

detectable orientations. Figure 12 shows simulation results for the TA-I system directed to a planar reflector. The Figure shows the simulated measures of the three sensors for the orientation range of $\theta \in [-15^\circ, +15^\circ]$. The

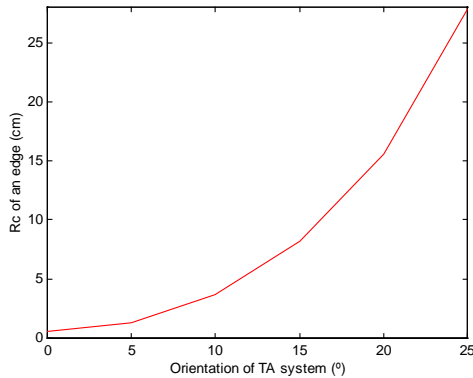


Figure 11. R_c vs Orientation of TA-I system

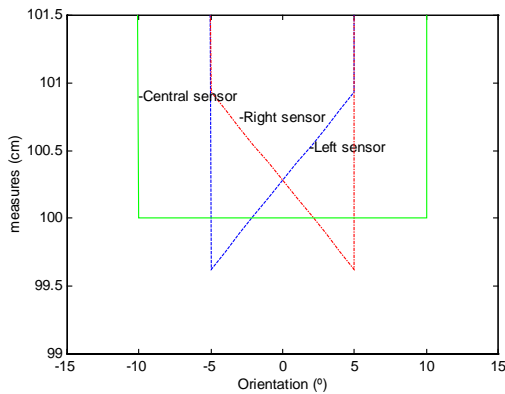


Figure 12. Measures of TA-I system vs θ orientation ($d=15$ cm; $r_l=100$ cm, $\phi=20^\circ$).

central sensor detects echoes in the orientation range of $\theta \in [-10^\circ, +10^\circ]$, while lateral sensors detect echoes only in the range of $\theta \in [-5^\circ, +5^\circ]$, consequently the detectable maximum orientation is 5° . In the TA-II system all three sensors detect echoes in the range of $\theta \in [-10^\circ, +10^\circ]$, in view of which, in this case, there is no dependency with the distance to the plane (reflector) and the optimum orientation bias of transducers is zero.

Varying the orientation angle of lateral transducers in the TA-I system it is possible to detect orientations of planar surfaces to the maximum range of $\theta \in [-10^\circ, +10^\circ]$, as it is shown in Figure 13. The area defined by the solid lines represents the orientation ranges detected using the measures of central and left sensors (equation 7). Using the central and right sensor measures, the orientation ranges as a function of ϕ defines the area limited by the dashed lines. Figure 13 shows that to the range of values of $\phi \in [+8^\circ, +15^\circ]$ corresponds the largest range of detected orientations of $\theta \in [-10^\circ, +10^\circ]$.

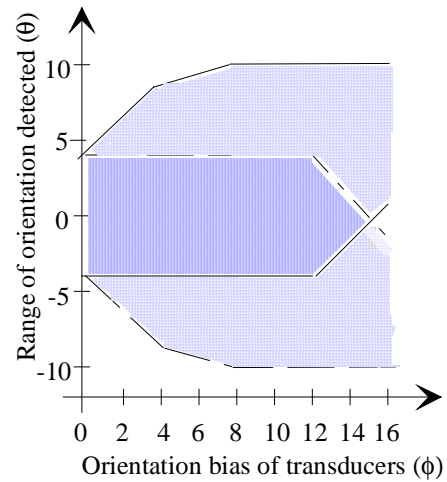


Figure 13. Orientations detected using equation 7 ($d=15$ cm; $r_l=75$ cm).

6 PRACTICAL APPLICATIONS

In this section we describe two experiments using the TA systems. The TA systems were configured in harmony with the results presented in the previous sections.

6.1 Surface Alignment

This task consists of the automatic aligning of the TA system with a planar reflector placed at an arbitrarily distance and orientation. The 2-DOF TA system moves in accordance to the TA sensors information in order to become parallel with the planar reflector at a desired distance from it. The results were very good using the models (7) (TA-I system) and (6) (TA-II system). The maximum alignment error experimentally observed was of about 1 degree.

Figure 14 shows detected orientations versus real orientations for a planar reflector placed at a distance of about 1 meter. As we can observe, the TA system is sufficiently accurate in the range of about $\pm 10^\circ$.

6.2 Mapping

This application consists of the recognition and localisation of objects placed randomly in a room. As shown in Figure 15, it was considered a set of four objects: a plane, an edge and two circular objects. Table 2 shows the results of a scanning of the environment using the TA-II system. The plane and the circular reflectors were recognised and localised with satisfactory accuracy. The edge was not recognised although it was well localised. Bad results with edges were already expected. In this case the ultrasound wave is diffracted resulting echoes emanating in all directions and therefore

characterised with very low amplitudes. Sonar map building was not achieved with TA-I system. In this case, the objects were only

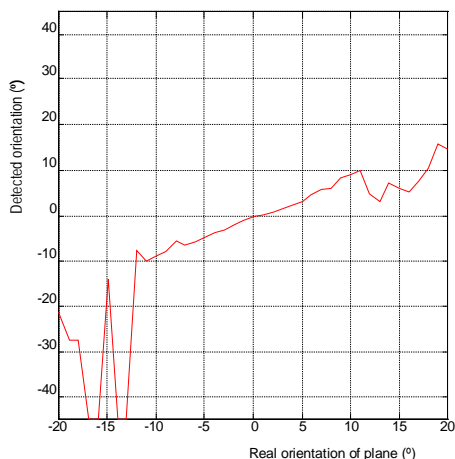


Figure 14. Detected orientations (model of equation 6).

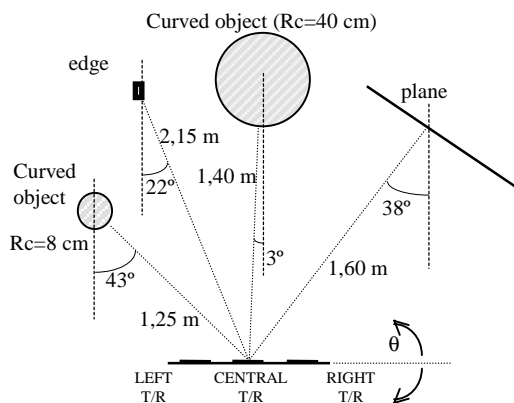


Figure 15. Top view of the environment used in the map building experiment.

recognised in the positions of $\theta=0$, and even so, not with good accuracy.

Table 2 Objects detected

Reflector	Rc measured	Orientation	Distance
Circular(R=8cm)	12 cm	-43°	126.9 cm
Edge	115 cm	-21°	217.2 cm
Circular(R=40 cm)	35 cm	3°	144.4 cm
Plane	1006 cm	37°	164.4 cm

7 CONCLUSION

In this paper two different systems have been presented and compared: TA-I and TA-II systems. For each one formulas were deduced that theoretically allow us to find the radius of curvature of an object and its localisation. It was verified that the TA-I system (equation 3) does not have good performance in practice. On

the other hand, the TA-II system has a good performance in practice allowing us to accomplish with success two practical applications: planar surface alignment and sonar map building. The geometric configuration of TA system is an important factor for improving the TA system performance in the recognition and localisation of objects.

REFERENCES

- [1] H. Peremans, K. Audenaert and J.M. Van Campenhout "A high-resolution sensor based in tri-aural perception", *IEEE Trans. on Robotics and Automation*, vol. 9, pp-36-48, February 1993.
- [2] Omur Bozma and Roman Kuc "Building a sonar map in a specular environment using a single mobile sensor", *IEEE Trans. PAMI*, Vol. 13, no 12, December 1991.
- [3] A. Sabatini "Ultrasound-based active hearing techniques for tracking and identification of objects", *IEEE ISIC'92*.
- [4] B. Barshan and Roman Kuc "Differentiating Sonar Reflections from Corners and Planes by Employing an Intelligent Sensor", *IEEE Trans. on PAMI*, Vol. 12, no 6, June 1990
- [5] A. Sabatini and O. Di Benedetto "Spatial localisation using sonar as a control point matching task", *Proc. of the 3rd Int. Symp. on Intelligent Robotic Systems '95*
- [6] O. Di Benedetto and A. M. Sabatini, "A system for robot continuous localisation using sonar", *Proc. of the 3rd Int. Symp. on Intelligent Robotic Systems '95*
- [7] P. Mckerrow, "Echolocation-From range to outline segments", *Int. Journ. Robotics and Autonomous Systems* 11(1993) 205-211.
- [8] Roman Kuc and Victor Brian Viard, "A physically based navigation strategy for sonar-guided vehicles", *The International Journal of Robotics Research*, vol. 10, no. 2, April 1991
- [9] Billur Barshan, "A bat-like sonar system for obstacle localisation", *IEEE Trans. SMC*, Vol. 22, no 4, July/August 1992.

